Available online at www.sciencedirect.com
SCIENCE DIRECT
Agricultural and Forest Meteorology 132 (2005) 212–227
AGRICULTURAL AND FOREST METEOROLOGY
www.elsevier.com/locate/agrformet

Continuous measurements of soil respiration with and without roots in a ponderosa pine plantation in the Sierra Nevada Mountains

Jianwu Tang [a,b,*], Laurent Misson [b], Alexander Gershenson [c], Weixin Cheng [c], Allen H. Goldstein [b]

[a] Department of Forest Resources, University of Minnesota, 1530 Cleveland Ave N, St. Paul, MN 55108, USA
[b] Department of Environmental Science, Policy, and Management, University of California at Berkeley, 151 Hilgard Hall, Berkeley, CA 94720, USA
[c] Department of Environmental Studies, University of California at Santa Cruz, 1156 High Street, Santa Cruz, CA 95064, USA

Received 19 May 2005; accepted 21 July 2005

Abstract

Continuous measurements of soil respiration and its components help us understand diurnal and seasonal variations in soil respiration and its mechanism. We continuously measured CO_2 concentration at various depths in the soil and calculated surface CO_2 efflux based on CO_2 gradients and diffusivity in a young ponderosa pine plantation in the Sierra Nevada Mountains of California. We determined soil respiration both in a control plot that included roots and in a trenched plot that had no roots. The difference between these plots was used to partition soil respiration into root respiration and heterotrophic respiration. We found that both CO_2 concentration in the soil and surface CO_2 efflux in the control plot were higher than in the trenched plot. The diurnal range of soil respiration in the trenched plot was larger than in the control. We observed dramatic pulses of soil respiration in response to rain events in summer and fall during the dry season. We modeled the seasonal variation in soil respiration without the pulses using soil temperature and moisture as driving variables and simulated soil respiration pulses using an exponential decay function in response to the volume of rain. Daily mean soil respiration peaked at 5.0 $\mu mol\ m^{-2}\ s^{-1}$ in the control and at 2.7 $\mu mol\ m^{-2}\ s^{-1}$ in the trenched plot in June before the rain pulses. Soil respiration increased from 4.9 to 8.2 and to 12.1 $\mu mol\ m^{-2}\ s^{-1}$ after the first and second rain events in the control, and increased from 2.2 to 4.1 and to 6.6 $\mu mol\ m^{-2}\ s^{-1}$ in the trenched plot. After incorporating the pulse effect, the model simulated measured data well. Annual soil respiration in 2003 was estimated as 1184 g C $m^{-2}\ y^{-1}$. The average ratio of root over total respiration was 0.56 during the growing season and 0.16 during the non-growing season with an annual average of 0.44.

Keywords: CO_2 efflux; CO_2 concentration; CO_2 gradient; Heterotrophic respiration; Pulse; Root respiration

1. Introduction

Soil surface CO_2 efflux, or soil respiration, has a potential role either to amplify global warming due to its sensitivity to environmental conditions (Cox et al., 2000; Trumbore et al., 1996; Kirschbaum, 2000), or to mitigate climate change due to enhanced soil carbon

* Corresponding author. Tel.: +1 612 624 5317; fax: +1 612 625 5212.
E-mail address: jtang@umn.edu (J. Tang).

0168-1923/$ – see front matter © 2005 Elsevier B.V. All rights reserved.
doi:10.1016/j.agrformet.2005.07.011

sequestration and reduced CO_2 efflux (Lal, 2004; Goh, 2004). Improved understanding of the mechanisms and quantification of the variations in soil respiration is essential for better managing these potentials. Because of the high temporal and spatial variations in soil respiration (Raich et al., 2002; Rayment and Jarvis, 2000; Law et al., 2001a; Tang and Baldocchi, 2005), high-resolution information on the local scale is necessary for evaluating the soil carbon budget on the global scale.

Soil respiration has been extensively measured using various methods. Chamber-based methods allow measurements of soil respiration on a small scale (e.g. Norman et al., 1992; Meyer et al., 1987). Portable chambers enable investigation of the spatial variation in soil respiration (Tang and Baldocchi, 2005). Automated chamber systems provide continuous and semi-continuous measurements for investigating the temporal variation in soil respiration (Russell et al., 1998; Scott et al., 1999; Goulden and Crill, 1997; Liang et al., 2003; Irvine and Law, 2002; King and Harrison, 2002; Drewitt et al., 2002). However, chamber-based measurements may create sampling biases by disturbing air pressure and altering CO_2 concentration in the soil (Livingston and Hutchinson, 1995; Healy et al., 1996; Davidson et al., 2002). Under-story eddy covariance methods provide an alternative to continuously measure soil CO_2 efflux without disturbing the soil (Baldocchi and Meyers, 1991; Law et al., 1999). However, the component flux from under-story vegetation often limits the use of under-story flux data and stable conditions make eddy covariance measurements in this environment difficult. The recently developed soil CO_2 vertical gradient measurement method provides an opportunity to measure soil respiration with high frequency (minutes to half hour) with minimum disturbance to the natural structure of the soil (Tang et al., 2003; Hirano et al., 2003; Liang et al., 2004; Jassal et al., 2005). This method has not been widely used earlier probably due to instrument limitations and difficulty in calculating soil surface CO_2 efflux from gradient measurements and CO_2 diffusivity in the soil.

Soil respiration has been widely simulated using continuous records of temperature, moisture, and other variables (e.g. Raich and Schlesinger, 1992; Davidson et al., 1998; Epron et al., 1999a; Xu and Qi, 2001; Treonis et al., 2002; Reichstein et al., 2003; Tang et al., 2005b). It has been observed that rainfall causes pulses of soil respiration and ecosystem respiration and that these pulse effects may significantly influence the annual carbon budget (Lee et al., 2004; Xu et al., 2004; Yuste et al., 2003). However, few models have incorporated the rain pulse effects in estimating the annual sum of soil respiration.

Partitioning soil respiration into root respiration (including associated respiration from mycorrhizae) and heterotrophic respiration helps us understand the mechanisms of soil respiration and aids in development of process-based carbon cycle models. The ratio of root respiration to total soil respiration may vary from 10 to 90% depending on vegetation type and season of the year (Hanson et al., 2000). In situ comparisons between soil respiration and heterotrophic respiration in a continuous and simultaneous way are rare, but are valuable for improving understanding of the different behavior between root respiration and heterotrophic respiration.

In this study, we report continuous measurements of CO_2 concentration gradients in the soil, provide an algorithm to calculate soil surface CO_2 efflux based on these gradients, quantify diurnal and seasonal patterns of soil respiration with roots (soil respiration) and without roots (heterotrophic respiration), and simulate seasonal variations in soil respiration and root respiration that include the rain pulse effects.

2. Materials and methods

2.1. Site description

The study site, a part of the Ameriflux and Fluxnet networks, is located in a young ponderosa pine (*Pinus ponderosa*) plantation (38°53′42.9″N, 120°37′57.9″W, 1315 m) adjacent to the University of California Blodgett Forest Research Station. The stand is dominated by ponderosa pine trees planted in 1990 after clear cutting. Douglas-fir (*Pseudotsuga menziesii*), white fir (*Abies concolor*), incense cedar (*Calocedrus decurrens*), giant sequoia (*Sequoiadendron giganteum*), and California black oak (*Quercus kelloggii*) occur sparsely in the overstory canopy. The major understory shrubs were *Arctostaphylos* spp. and *Ceonothus* spp.

The plantation had an original tree density of 1213 stems ha^{-1}. Shrubs were cut during spring 1999 and the plantation was thinned in May 2000 as a forest management practice. About 60% of trees and 30% of total biomass and leaf area including most shrubs were cut down and masticated into detritus (Tang et al., 2005b; Misson et al., 2005). In spring 2003, one-sided leaf area index (LAI) averaged 1.79 for the overstory and 0.7 for the understory shrubs. Stand density was 378 stems ha^{-1} with mean tree diameter at breast height (DBH) of 12.0 cm, mean tree height of 4.7 m, and basal area of 9.58 m^{-2} ha^{-1} in 2003.

The site is characterized by a Mediterranean climate with hot and dry summers, and relatively cold and wet winters. Since 1998, annual precipitation has averaged 1290 mm, with the majority of precipitation falling between September and May with very few rain events in summer. The site is periodically covered by snow in the winter. Daily mean temperature ranged from 14–27 °C during summer and from 0–9 °C during winter. Trees generally break bud in May and set bud in late July to early August. The growing season ranges from May to October.

The study site is relatively flat with slopes less than 3° in our sampling area. The soil is a fine-loamy, mixed, mesic, ultic haploxeralf in the Cohasset series whose parent material was andesitic lahar. It is relatively uniform and dominated by loam and sandy-loam with sand of 60%, silt of 28%, and clay of 12%. Coarse woody debris is scattered on the forest floor from the residues of previous harvest (clear-cutting) and thinning operations. The soil at 0–30 cm had an average organic matter content of 6.9%, and total nitrogen of 0.17% measured in 1998 (Xu and Qi, 2001).

Extensive carbon cycling studies have been conducted at this site including carbon flux (Goldstein et al., 2000), forest thinning (Tang et al., 2005b; Misson et al., 2005), photosynthesis (Misson et al., 2004) and soil respiration and ecosystem respiration based on chamber measurements (Xu et al., 2001; Xu and Qi, 2001). However, no continuous measurements of soil respiration have been published at this site.

2.2. Field measurements

We established two 20 m × 20 m sampling plots (control plot), 40 m away from each other within the footprint area of the Blodgett Forest AmeriFlux tower for flux measurements. We installed 18 soil collars, with a height of 4.4 cm and a diameter of 11 cm, on two 3 × 3 matrixes in the two plots for chamber measurements of soil respiration. Periodical measurements of soil respiration were made each month with a LI6400-09 soil chamber connected to a LI-6400 portable photosynthesis system (LI-COR Inc., Lincoln, NE) for data collection and storage. Soil temperature at 10 cm depth were continuously measured adjacent to the soil collars. Volumetric soil moisture at 0–30 cm depth was measured at the center of each plot. We used custom-built thermocouple sensors to monitor soil temperature, and time domain reflectometry probes (TDR, CS615 Campbell Scientific Inc., Logan, UT) inserted vertically into the soil to monitor volumetric soil moisture. Dataloggers (CR10X and 23X, Campbell Scientific Inc., Logan, UT) were programmed to store temperature and moisture data every 5 min. In addition, air temperature, precipitation, soil temperature in three locations at 5, 10, 15, 30 and 50 cm depths, soil moisture at 10, 30 and 50 cm depths, and other meteorological parameters were also measured and stored as half-hour averages at the nearby AmeriFlux tower (Goldstein et al., 2000).

We selected a relatively open space and established a small plot (trenched plot) of 3 m × 3 m about 30 m away from the center of the western control plot in July 2001 for a trenching experiment. There were no trees inside the plot, and nor tree shading for the plot. We dug a trench 0.2 m wide and 1.2 m deep around the plot. After lining the trench with polyethylene sheets, we refilled the soil back into the trench according to its original soil profiles while minimizing disturbance as much as possible. The trenching cut down most live roots that extended into the plot. The plot was then kept free of seedlings and herbaceous vegetation by periodic manual removal. Thus, we assumed there were no root influences within this plot. We installed two soil collars in the trenched plot for chamber measurements of soil respiration. We also installed two soil thermocouple sensors at 10 cm and a moisture sensor (TDR, CS615 Campbell Scientific Inc., Logan, UT) at 0–30 cm for continuously measuring soil temperature and moisture at 5 min intervals.

Continuous soil respiration was assessed using soil CO_2 gradient measurement systems. In early May 2003, we buried two sets of solid-state infrared gas analyzers (GMT 222, Vaisala Inc., Finland), one at the center of the western control plot and the other at the trenched plot, at 2, 8 and 16 cm depths to measure CO_2 concentration vertical profiles in the soil continuously, similarly to the deployment described in detail by Tang et al. (2003). The sensor probes were cased with PVC pipes that had the same length but were 5 mm larger in diameter, and vertically buried in the soil. The casings were sealed with the probe on the upper end, allowing CO_2 molecules to diffuse to the sensors at the lower end at a certain depth. For further protection from water, the sensors were coated with Gortex-type fabric that allowed gaseous CO_2 to diffuse in but excluded liquid water. The sensors were placed 1 m away from the soil collars for complementary chamber measurements. Soil temperatures were measured with thermocouples at depths of 2, 8 and 16 cm adjacent to the soil CO_2 gradient measurements. The CO_2 and temperature profile measurements were taken every 30 s and then stored as 5-min averages on a datalogger (CR-23X, Campbell Scientific Inc., UT). The technical specifica-

tions indicate that the accuracy of the CO_2 sensors is ± 20 μmol mol^{-1} plus 2% of reading. We calibrated the sensors using lab standards that are traceable to the NOAA/CMDL standards, and found that the shift of spans were in the specification range. We took away the CO_2 sensors from the field in November before snow occurred while leaving the temperature sensors in the field for the winter.

2.3. CO_2 gradient data analysis

CO_2 concentration measurements by the CO_2 sensors were corrected for variations in temperature and pressure (Tang et al., 2003) and used to calculate the surface CO_2 efflux.

The data from the CO_2 sensors constitute the volume fraction C_v (μmol mol^{-1}). Volume fraction can be changed to mole concentration by:

$$C = \frac{C_v P}{RT} \tag{1}$$

where C is the mole concentration (μmol m^{-3}), C_v the volume fraction (μmol mol^{-1}), P the air pressure (Pa), T the soil absolute temperature (K), and R the universal gas constant (8.3144 J mol^{-1} K^{-1}).

The flux of CO_2 at depth z was calculated by Fick's first law of diffusion:

$$F_z = -D_s \frac{dC}{dz}, \tag{2}$$

where F_z is the CO_2 efflux (μmol m^{-2} s^{-1}), D_s the CO_2 diffusivity in the soil (m^2 s^{-1}), C the CO_2 mole concentration at a certain depth of the soil (μmol m^{-3}), and z the depth (m). The negative sign indicates that the efflux is in the direction of decreasing concentration.

Diffusivity was computed using the recently developed Moldrup model (Moldrup et al., 1999), which applies to various undisturbed soils.

$$\frac{D_s}{D_a} = \phi^2 \left(\frac{\varepsilon}{\phi}\right)^{\beta S} \tag{3}$$

where D_a is the CO_2 diffusivity in free air, and the effect of temperature and pressure on D_a is given by:

$$D_a = D_{a0} \left(\frac{T}{T_0}\right)^{1.75} \left(\frac{P_0}{P}\right), \tag{4}$$

where T is the temperature (K), P the air pressure (Pa), D_{a0} a reference value of D_a at T_0 (293.15 K) and P_0 (1.013×10^5 Pa), and is given as 1.47×10^{-5} m^2 s^{-1} (Jones, 1992).

ε is the volumetric air content (air-filled porosity), ϕ the porosity or sum of the volumetric air content ε and the volumetric water content θ. Note,

$$\phi = 1 - \frac{\rho_b}{\rho_m} = \varepsilon + \theta, \tag{5}$$

where ρ_b is the bulk density (0.58 g cm^{-3} at the control plot and 0.75 g cm^{-3} at the trenched plot measured with soil cores at 0–20 cm), and ρ_m the particle density for the mineral soil, with a typical value of 2.65 g cm^{-3}. ϕ (0.78 at the control plot and 0.72 at the trenched plot) does not change with time while ε changes with soil water content over time. S is the percentage of mineral soil with size >2 μm, or S = silt + sand content. $S = 0.88$ at our site. $\beta = 2.9$ is a constant.

Combining Eqs. (1)–(5), we can compute CO_2 flux (F_z) at the depth of z in the soil:

$$F_z = -\left(\frac{D_{a0} P_0 \phi^2}{R T_0^{1.75}}\right)\left(\frac{\phi - \theta}{\phi}\right)^{2.9S} T_z^{1.75} \frac{d(C_{vz}/T_z)}{dz} \tag{6}$$

where T_z and C_{vz} are the temperature and CO_2 volume fraction, respectively, at the depth of z. Eq. (6) indicates that at a specific site, F_z is a function of soil temperature, soil moisture (water content) and CO_2 concentration (volume fraction).

At a certain small layer of soil if we measure CO_2 concentration at the depth of z_i and z_{i+1} with concentration C_i and C_{i+1}, Eq. (6) can be approximated assuming a constant flux rate within this layer:

$$F_i = -\left(\frac{D_{a0} P_0 \phi^2}{R T_0^{1.75}}\right)\left(\frac{\phi - \theta}{\phi}\right)^{2.9S} \left(\frac{T_i + T_{i+1}}{2}\right)^{1.75} \times \left(\frac{C_{i+1}/T_{i+1} - C_i/T_i}{z_{i+1} - z_i}\right) \tag{7}$$

where F_i is the CO_2 flux (μmol m^{-2} s^{-1}) between depth z_i and z_{i+1} (m), T_i and T_{i+1} are the temperature (K) at the depths of z_i and z_{i+1}, C_i and C_{i+1} the CO_2 concentration (μmol mol^{-1}) at the depths of z_i and z_{i+1}, ϕ is the soil porosity, θ the volumetric water content between the depth z_i and z_{i+1}, S the sum of silt and sand content, and constants $D_{a0} = 1.47 \times 10^{-5}$ m^2 s^{-1}, $R = 8.3144$ J mol^{-1} K^{-1}, $T_0 = 293.15$ K, and $P_0 = 1.013 \times 10^5$ Pa. Notice, the depth z is in the negative sign when it is

an input for an equation, but we omit the negative sign when we describe the soil depth in the text.

It is difficult to measure CO_2 concentration at the boundary of the soil and atmosphere ($z = 0$). We measured CO_2 concentration at the depth of 0.02, 0.08 and 0.16 m and thus we calculated CO_2 fluxes between 0.02 and 0.08 m and between 0.08 and 0.16 m based on Eq. (7). Since we have only two flux measurements at two depths, CO_2 flux at the surface (F_0) was linearly extrapolated based on Eq. (8), assuming CO_2 production (the slope of F against z) in the soil shallow layers (0–0.2 m) was a constant:

$$F(z) = pz + F_0 \tag{8}$$

where $F(z)$ is the CO_2 flux (μmol m^{-2} s^{-1}) at any depth z, p the CO_2 production (μmol m^{-3} s^{-1}, the source term including that from roots and microbes), z the depth (m) and $-0.2\ \text{m} < z < 0$, and F_0 (μmol m^{-2} s^{-1}) the CO_2 flux at the surface (when $z = 0$).

The assumption of constant CO_2 production did not hold during some transient periods such as the sudden rain events during a long dry summer. These rain events may only wet the surface litter and the very shallow soil but stimulate CO_2 efflux pulses (Xu et al., 2004). During these short periods, CO_2 concentration gradients in the soil may be inversed with higher concentrations at the shallow layers, and CO_2 production near the surface (around 0.02 m) may be the major contribution to surface CO_2 efflux. In this situation, we used an approximate method by using Eq. (7) to calculate F_0 based on CO_2 concentration at 0.02 m belowground and atmospheric CO_2 concentration close to the ground. We used atmospheric CO_2 concentration at 0.5 m obtained from atmospheric CO_2 vertical profile measurements with a closed-path infrared gas analyzer (LI-6262, LI-COR Inc., Lincoln, NE) at the adjacent under-story eddy covariance tower (Misson et al. in preparation) to approximate the atmospheric CO_2 concentration close to the ground. Though CO_2 concentration close to the ground may be higher than that at 0.5 m aboveground (averaged 370 μmol mol^{-1}), the error (overestimation of CO_2 efflux) associated with this approximation in calculating the gradient was small considering high CO_2 concentration measurements at 0.02 m belowground (>6000 μmol mol^{-1}) during these short transient periods (a few hours) after the rain.

2.4. Modeling soil respiration

To model soil respiration averaged over the site, continuously determined soil respiration based on CO_2 gradients from the control plot, which represented a point measurement, was adjusted by periodical chamber measurements with 18 spatial samples to reflect site-averaged soil respiration. We plotted simultaneous measurements of soil respiration from chamber against from gradient methods, established a linear relationship between the site-average and point measurements (Fig. 1). We used this relationship to correct continuous soil respiration from gradient measurements for representing the site-average. Similarly, continuously determined soil respiration from the trenched plot was also adjusted by chamber measurements from two soil collars in the trenched plot. The adjusted soil respiration data were used to parameterize a soil respiration model with inputs from soil temperature and moisture.

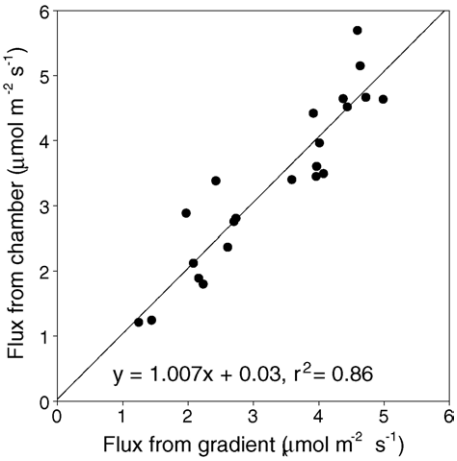

Fig. 1. Simultaneous measurements of soil respiration from chamber against from gradient methods in the control plot. Chamber measurements were averages over 18 point measurements during D126–D330.

Soil respiration was controlled both by soil temperature and moisture in this Mediterranean-type ecosystem. We therefore developed a model using two independent variables, soil temperature and moisture, to simulate temporal variation of soil respiration, similar to that reported by Tang et al. (2005b):

$$F = \beta_0 e^{\beta_1 T} e^{\beta_2 \theta + \beta_3 \theta^2} \tag{9}$$

where F (μmol m^{-2} s^{-1}) is the soil respiration, T (°C) the soil temperature at 10 cm depth, θ (m^3 m^{-3}) the soil volumetric moisture for the 0–30 cm soil layer, and β_0, β_1, β_2, and β_3 are the model coefficients. Eq. (9) can be log-transformed to a linear model. The quadratic-type form of θ indicates that soil moisture has two opposite effects on soil respiration. By conducting multivariate linear regression analysis with the statistical package

Stata (Stata Corporation, Texas), we estimated the model coefficients.

We observed significant pulses of soil respiration after the first and second rain in the summer–fall period, similar to those seen by Xu et al. (2004) and Jassal et al. (2005). The increase in soil moisture alone could not reproduce the observed pulses using our parameterized model. In addition to Eq. (9), which adequately described soil respiration during most days of the year, we developed a model simulating the pulses of soil respiration caused by rain.

We found the decay of soil respiration after the rain pulse in the dry season followed an exponential decay function, similar to the result of Xu et al. (2004) in a grassland and savanna in the Sierra Nevada foothills characterized by a Mediterranean climate:

$$F_R = F_b + ae^{-t/\tau} \quad (10)$$

where F_R (μmol m^{-2} s^{-1}) is the soil respiration after the rain, F_b (μmol m^{-2} s^{-1}) the soil respiration before the rain, or the baseline of soil respiration before the pulse, t (day) the time since the rain, the coefficient a (μmol m^{-2} s^{-1}) indicates the peak pulse above the baseline F_0 when $t = 0$, and the coefficient τ (day) indicates the decay speed and represents the time required for F_R above F_b to decline to $1/e$ (e is the base for natural log; $1/e \sim 0.37$) of its peak value a.

We found that a is proportional to the daily sum of rain:

$$a = a_0 + kP_R \quad (11)$$

where P_R (mm) is the amount of rain, and coefficients a_0 and k varied between the control and trenched plots. Eq. (10) was only used to simulate the first and second rain during the summer–fall when the observed pulses of CO_2 efflux were substantial.

Two sets of parameters in Eqs. (9)–(11) were fitted for the control plot and the trenched plot, respectively, based on measurement data. The parameters for the trenched plot were used to estimate heterotrophic respiration in the control plot. The difference between heterotrophic respiration and soil respiration in the control plot was root respiration. We used site-averaged soil temperature at 10 cm and soil moisture at 0–30 cm on a daily scale to drive the models and estimate the annual sum of soil respiration, heterotrophic respiration, and root respiration. Eq. (9) was used to estimate daily mean soil respiration and heterotrophic respiration except on days with rain-induced respiration pulses. Eq. (10) was used to estimate respiration pulses following the first and second rain events during the summer–fall (days of year 215–260) when the soil was dry.

3. Results

3.1. Diurnal and daily variations in CO_2 concentration in the soil

Fig. 2 shows the diurnal variations in soil CO_2 concentration measured on day of year (D)153, D183, D214, D244, D275 and D307, demonstrating the monthly change of the diurnal patterns from early June (D153) to early November (D307). On D153 CO_2 concentration averaged 1270, 2920, and 6120 μmol mol^{-1} at 2, 8, and 16 cm, respectively, in the control plot, greater than the concentrations in the trenched plot, which averaged 1000, 2360, and 5300 μmol mol^{-1} at 2, 8, and 16 cm, respectively. However, the diurnal range in the trenched plot was larger than the control. The deeper soil had a larger diurnal range of CO_2 concentration than the surface soil, even though the deeper soil had a small diurnal range of soil temperature (data now shown). CO_2 concentration peaked around 21–23 h in the control and around 17–19 h in the trenched plot.

The diurnal ranges of soil CO_2 concentration were larger in June than later months (excluding D214 with rain pulse effects). The first rain in the summer–fall occurred on D212 with a sum of 1.8 mm, followed by the rain of 11.4 mm on D214, starting from early morning. CO_2 concentrations immediately responded to the rain and increased substantially on D214. Within a day CO_2 concentrations increased by 950, 1730, and 1600 μmol mol^{-1} at 2, 8, and 16 cm, respectively, in the control. CO_2 concentration increased more significantly in the trenched plot with increases of 3700, 3130, and 2030 μmol mol^{-1} at 2, 8, and 16 cm, respectively.

On D244 CO_2 concentration was still high at all depths, influenced by the rain of 5.1 mm a day before and by the rain of 19.6 mm during D233–D238. CO_2 concentration substantially decreased in October and early November. On D307 CO_2 concentrations were close to D275. Although there was a rain of 12.4 mm on D307, we did not see any pulse of CO_2 concentration in early November when consecutive rain occurred and soil moisture increased dramatically.

3.2. Diurnal and daily variations in soil respiration

Diurnal variations in soil respiration in the control and trenched plot on six days from June to November

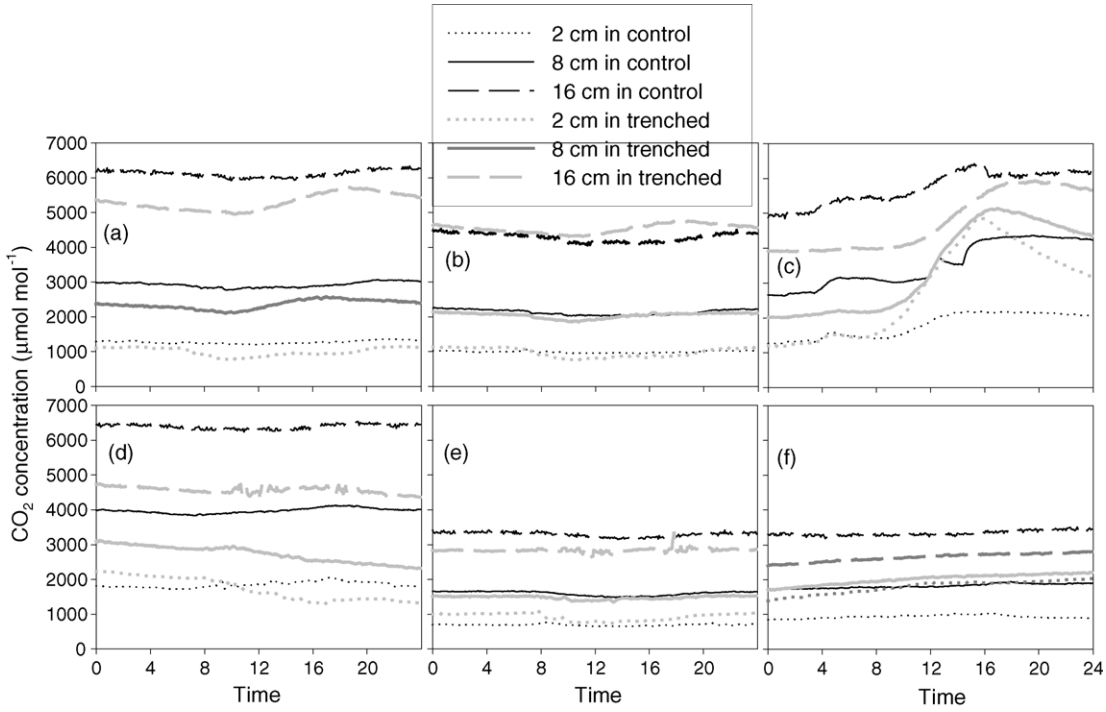

Fig. 2. Diurnal variations in CO_2 concentration measurements in the soil on: D153 (a); D183 (b); D214 (c); D244 (d); D275 (e); and D307 (f). The dot line, solid line and dash line indicate CO_2 concentration at 2, 8, and 16 cm, respectively. The black lines are for the control plot, and gray lines are for the trenched plot.

are shown in Fig. 3, as a combined result from gradients of CO_2 concentration in the soil shown in Fig. 2 and soil diffusivity. CO_2 efflux from the control was larger than from the trenched plot, but the diurnal range of CO_2 efflux was larger in the trenched than in the control. On D153, CO_2 efflux in the control increased slightly in the morning from 4.3 μmol m^{-2} s^{-1} to a maximum of 5.0 μmol m^{-2} s^{-1} in the afternoon with a daily average of 4.7 μmol m^{-2} s^{-1}, while CO_2 efflux in the trenched plot increased from 1.8 μmol m^{-2} s^{-1} in the early

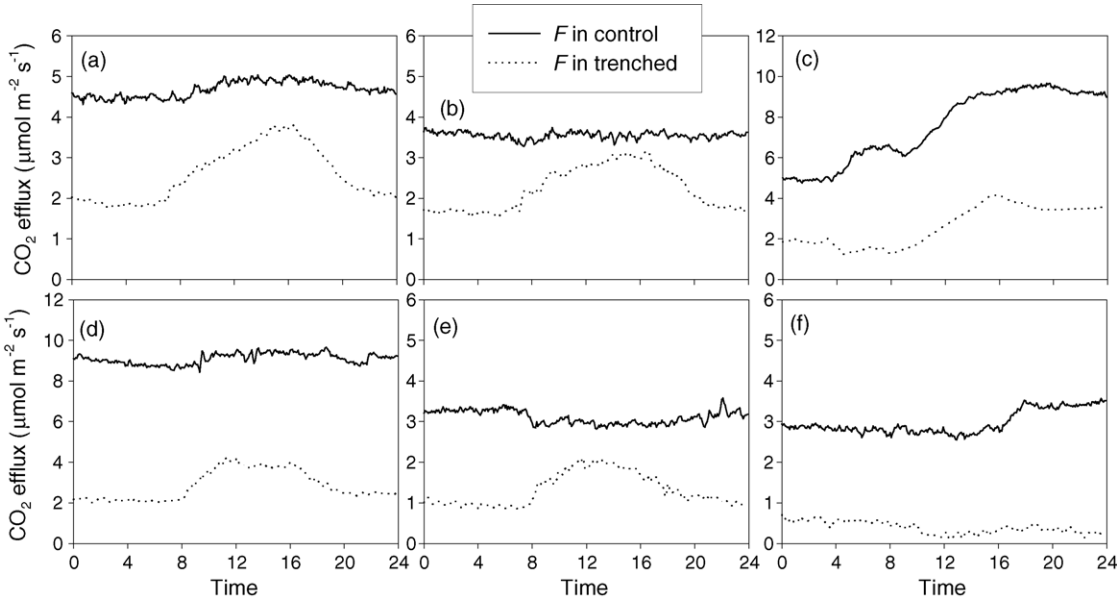

Fig. 3. Diurnal variations in soil respiration in the control and trenched plots on: D153 (a); D183 (b); D214 (c); D244 (d); D275 (e); and D307 (f).

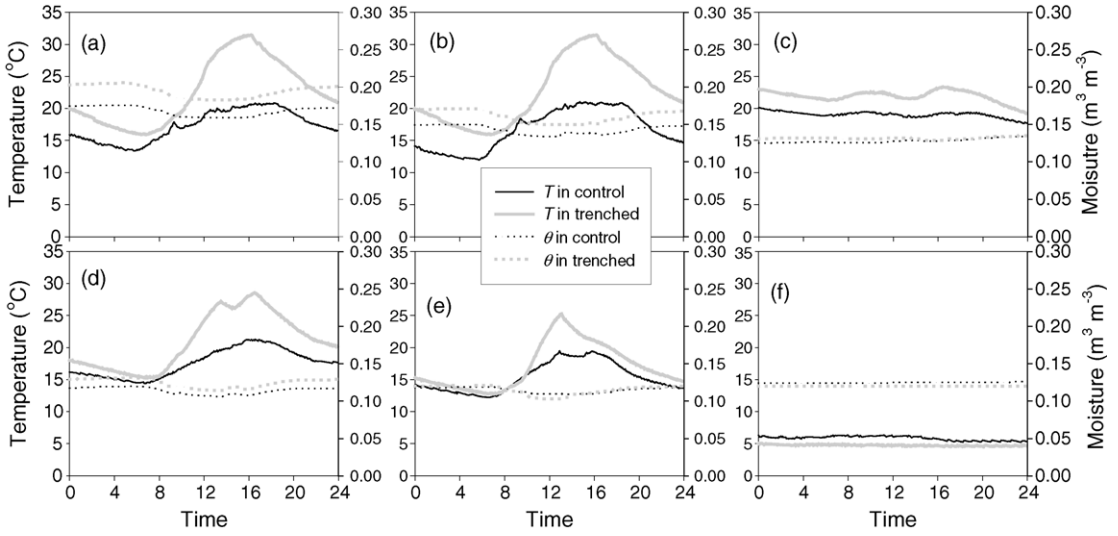

Fig. 4. Diurnal variations in soil temperature at 8 cm and soil moisture at 0–30 cm in the control and trenched plots on: D153 (a); D183 (b); D214 (c); D244 (d); D275 (e); and D307 (f). The solid lines are temperature and dotted lines are moisture. The black lines are for the control plot, and gray lines are for the trenched plot.

morning to a peak of 3.8 μmol m^{-2} s^{-1} around 16 h with a daily average of 2.6 μmol m^{-2} s^{-1}. On D183, the daily average of CO_2 efflux in the control decreased to 3.5 μmol m^{-2} s^{-1} with a small range of 0.5 μmol m^{-2} s^{-1}; the daily average in the trenched plot also decreased to 2.2 μmol m^{-2} s^{-1} with a diurnal range decreased to 1.6 μmol m^{-2} s^{-1} compared to 2.0 μmol m^{-2} s^{-1} on D153.

CO_2 efflux increased dramatically on D214 following the rain, from 4.9 to 9.7 μmol m^{-2} s^{-1} in the control, and from 1.2 to 4.2 μmol m^{-2} s^{-1} in the trenched plot during the day. CO_2 efflux decreased from D244 to D275 and D307. D244 was in the period of the second rain pulses following the rain during D233–D243. The daily average of CO_2 efflux was 9.1, 3.1, and 3.0 μmol m^{-2} s^{-1} on D244, D275, and D307, respectively, in the control, and 2.8, 1.3 and 0.4 μmol m^{-2} s^{-1} on D244, D275, and D307, respectively, in the trenched plot. D307 was a rainy day at the beginning of the wet season and CO_2 efflux showed a small increase in the afternoon in the control but not in the trenched plot.

Fig. 4 shows diurnal variations in soil temperature at 8 cm and soil moisture at 0–30 cm on six days. Overall, soil temperature in the trenched with no tree shading was higher both in daily average and diurnal range than in the control. Soil moisture was higher in trenched plot than in the control on D153 and D183 before the rain. After the rain, soil moisture in the trenched plot was similar to that in the control.

The combination of soil temperature and moisture explained most of the diurnal variation and seasonal variation of CO_2 efflux. The higher diurnal range of soil temperature in the trenched plot than that in the control corresponded with higher diurnal range of soil CO_2 efflux in the trenched plot. Except for the rain influence on D214 and D307, high soil temperature in the afternoon correlated with high CO_2 efflux in the trenched plot, but this correlation was not strong for the control plot. During the summer drought, soil moisture at 0–30 cm decreased from 0.17 m^3 m^{-3} on D153 to 0.14 m^3 m^{-3} on D183 in the control, and from 0.19 m^3 m^{-3} on D153 to 0.16 m^3 m^{-3} on D183 in the trenched plot, while soil temperatures on these two days were similar (Fig. 4a and b). This decrease in soil moisture at constant temperature corresponded with a decrease in soil CO_2 efflux from D153 to D183. Soil moisture averaged at 0–30 cm did not reflect the first rain on D214 when only the very shallow soil may be wetted. Similarly, the rain before D244 did not substantially increase soil moisture at 0–30 cm. However, high soil CO_2 efflux on D244 occurred despite the relatively low soil temperature. On D275 low soil CO_2 efflux corresponded with low soil temperature compared with D153 and D183. Low temperature also corresponded with low soil CO_2 efflux on D307 in both plots.

3.3. Seasonal variations in soil respiration

Continuous measurements of daily mean CO_2 efflux, soil temperature at 8 cm, soil moisture at 0–30 cm and rainfall, and diffusivity for CO_2 in the soil in the

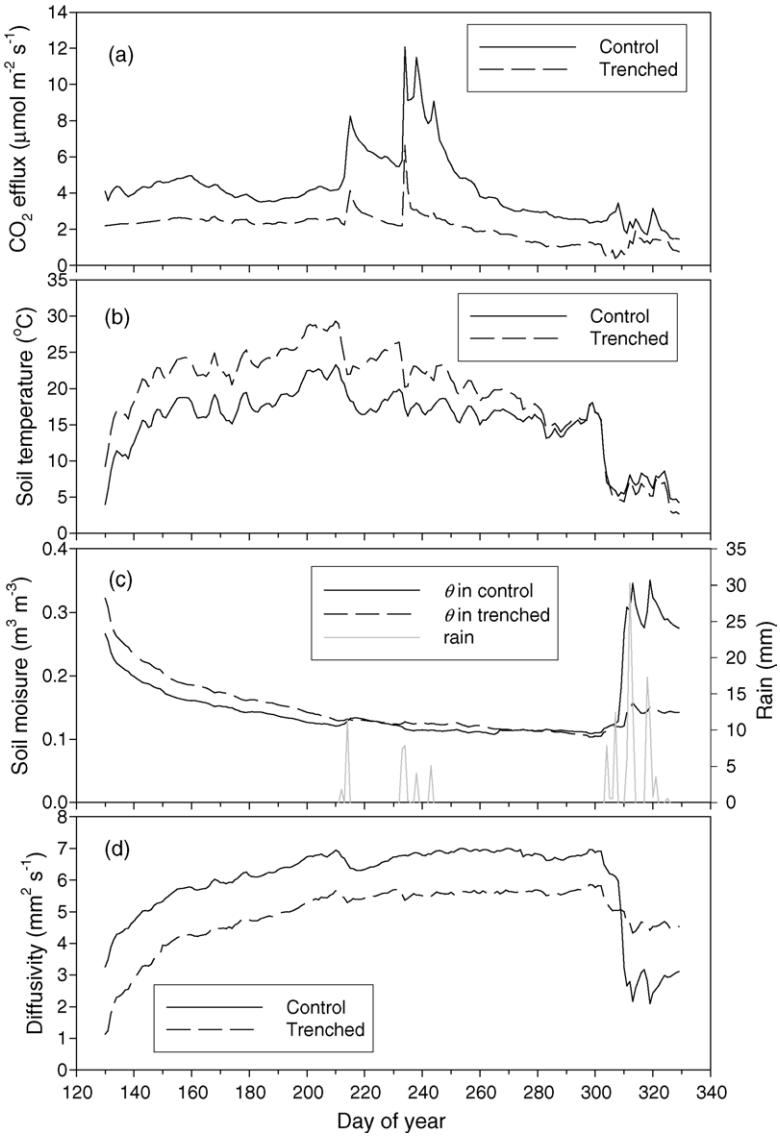

Fig. 5. Daily mean CO_2 efflux (a); soil temperature at 8 cm (b); soil moisture at 0–30 cm and rainfall (c); and diffusivity for CO_2 in the soil (d) in the control and trenched plots.

growing season in the control and trenched plot are shown in Fig. 5. Soil respiration increased in May and early June, and slightly decreased in late June (Fig. 5a). Two summer rain events in August dramatically increased CO_2 efflux. Soil respiration in the control increased from 4.9 μmol m^{-2} s^{-1} on D213 before rain to 8.2 μmol m^{-2} s^{-1} on D215 following 11.4 mm of rain on D214, and then increased to 12.1 μmol m^{-2} s^{-1} on D234 following 15.2 mm of rain. Soil respiration in the trenched plot also increased from 2.2 μmol m^{-2} s^{-1} on D213 before rain to 4.1 μmol m^{-2} s^{-1} on D215, and then increased to 6.6 μmol m^{-2} s^{-1} on D234. The fall–winter rain after these two rain events still caused small pulses but much less substantial than the first two rain events. Before the rain pulse, soil CO_2 efflux in the control peaked at 5.0 μmol m^{-2} s^{-1} on D159, while soil CO_2 efflux in the trenched plot peaked at 2.7 μmol m^{-2} s^{-1} on D168. High soil CO_2 efflux around D159–D168 was consistent with relatively high soil temperature and moderate soil moisture, which provided an optimal condition for tree growth as well as for soil respiration.

Soil temperature in the trenched plot was higher than in the control until late October when soil temperature in the control with canopy shading became higher (Fig. 5b). Daily mean soil temperature peaked at 23.3 °C in the control and 29.3 °C in the trenched plot

on D210. Soil moisture at 0–30 cm continuously decreased from May to October before the wet season in the winter–spring with a minimum of 0.11 $m^3\ m^{-3}$ in the control and 0.10 $m^3\ m^{-3}$ in the trenched plot (Fig. 5c). Soil moisture in the trenched plot was higher than in the control starting in May but this pattern switched in early October. Two rain events during D212–D214 and D233–D243 did not substantially increase soil moisture at 0–30 cm, but soil moisture increased rapidly after heavy rain around D312. Soil moisture in the control increased faster than in the trenched plot in the fall–winter. The restriction of soil moisture in the trenched plot could be related to the lack of rainfall interception by leaves and branches and thus more surface runoff during rainfall.

Diffusivity for CO_2 in the soil varied over the season (Fig. 5d). Soil diffusivity increased from the spring to fall, corresponding with the decrease in soil moisture. Soil diffusivity in the control was higher than the trenched plot, corresponding with lower soil moisture in the control. Daily mean soil diffusivity peaked at 7.00 $mm^2\ s^{-1}$ in the control and 5.86 $mm^2\ s^{-1}$ in the trenched plot. The rain events in August slightly reduced diffusivity. Soil diffusivity dramatically decreased in early November, when consecutive rain occurred. In the wet season, diffusivity in the control was lower than in the trenched plot, corresponding with higher soil moisture in the control.

3.4. Modeled soil respiration and root respiration

We simulated soil CO_2 efflux using the model driven by soil temperature, moisture, and precipitation. Eq. (9) was used to simulate most of the variation in CO_2 efflux except during the period of the pulses in response to rain events. The rain pulse model (Eqs. (10) and (11)) was used to simulate the pulse effect and its decay during D215–D260. Table 1 shows the coefficients for Eqs. (9)–(11) and their r^2 and sample size (n) in the control and trenched plot. We used only two rain events ($n = 2$) for estimating a_0 and k, and we modeled only these two rain pulses.

Table 1
Coefficients for Eqs. (9)–(11) and their r^2 and sample size (n) in the control and trenched plot

Equation	Coefficient	Control	Trenched
$F = \beta_0 e^{\beta_1 T} e^{\beta_2\theta+\beta_3\theta^2}$	β_0	0.582	0.141
	β_1	0.039	0.057
	β_2	13.367	13.355
	β_3	−31.415	−19.777
	r^2	0.71	0.79
	n	154	154
$F_R = F_b + ae^{-t/\tau}$	τ	5.599	3.521
	r^2	0.95	0.90
	n	46	46
$a = a_0 + kP_R$	a_0	−8.183	−6.078
	k	1.011	0.713
	r^2	1.0	1.0
	n	2	2

Fig. 5a and b show modeled CO_2 efflux versus measurements with and without pulse effects in the control and trenched plots, respectively. Adding the simulation of rain effects, the model results explained the measurement data well, with $r^2 = 0.88$ for the control and $r^2 = 0.68$ for the trenched plot. Without the simulation of rain effects, the model, which incorporated only soil temperature and moisture as driving

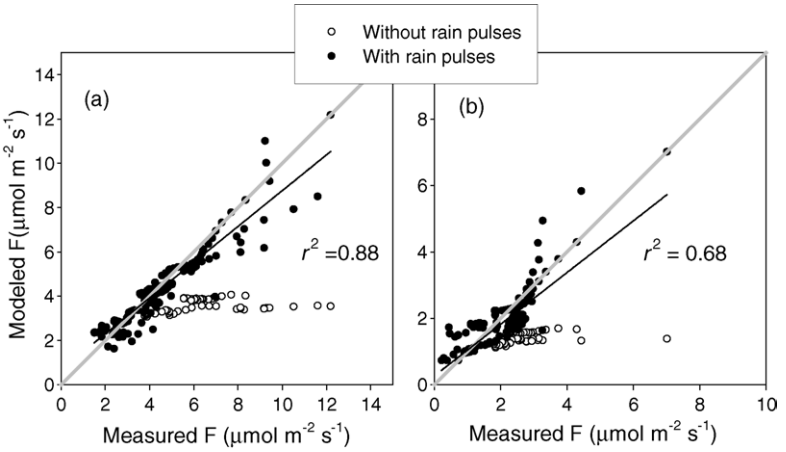

Fig. 6. Modeled CO_2 efflux vs. measurements with and without rain pulses in the control (a) and trenched plots (b). The black lines are fitted for the models with rain pulses. The gray lines are $y = x$.

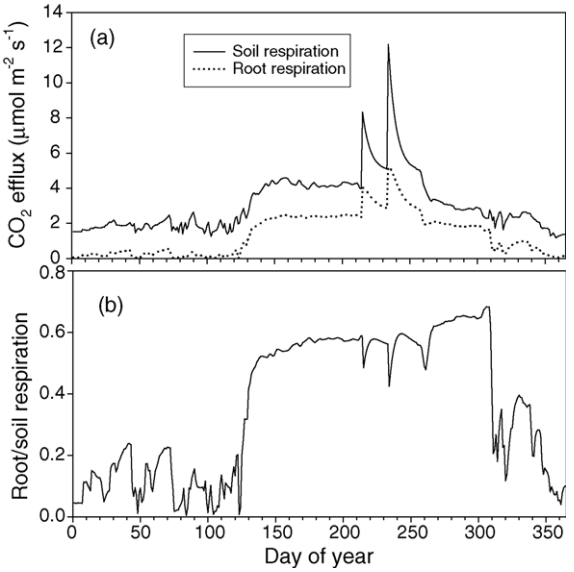

Fig. 7. Modeled results for daily mean soil respiration, root respiration (a) and the ratio of root respiration to soil respiration (b) during year 2003.

variables, had $r^2 = 0.18$ for the control and $r^2 = 0.27$ for the trenched plot and failed to explain high measurement values that occurred after the first and second rain in the summer and fall.

We plotted modeled results of daily mean soil respiration, root respiration, and the ratio of root over soil respiration during year 2003 (Fig. 7a and b). Soil respiration and root respiration had a small variation in the winter with an average of 1.83 and 0.21 μmol $m^{-2}\,s^{-1}$ for soil respiration and root respiration, respectively. Respiration increased after D120. Excluding the pulse effect caused by rain, daily mean soil respiration peaked at 4.58 μmol $m^{-2}\,s^{-1}$ on D158, and root respiration peaked at 2.48 μmol $m^{-2}\,s^{-1}$ on D201. The model simulated the rapid increase in soil respiration, and the subsequent decay of the efflux pulse following rain. Daily mean soil respiration peaked at 8.33 μmol $m^{-2}\,s^{-1}$ (almost twice its previous basal value) for the first pulse on D215, and peaked at 12.19 μmol $m^{-2}\,s^{-1}$ (triple its basal value) for the second pulse on D234. Root respiration correspondingly increased during the pulse but not proportionally to soil respiration, with increasing ratios of 1.7 and 2.2 over its basal value. There were no significant pulses following the rain in the fall and winter when soil moisture was high. The annual sum of soil respiration was estimated as 1184 g C $m^{-2}\,y^{-1}$, with root respiration estimated as 524 g C $m^{-2}\,y^{-1}$.

The ratio of root to soil respiration (F_r/F) varied seasonally (Fig. 7b). The F_r/F ratio substantially increased after D125, indicating the season with fast growth of roots. During the rain pulse period, F_r/F decreased due to stronger rain pulses for soil respiration than for root respiration. F_r/F substantially decreased after D310, suggesting the end of the root growing season. The average of F_r/F was 0.56 during the growing season and 0.16 during the non-growing season with an annual average of 0.44.

4. Discussion

4.1. CO_2 concentration and flux

CO_2 concentration in a certain layer of the soil, which we measured, is a state variable generally resulting from production of CO_2 (including that from microbes and from roots) in this layer, inflow of CO_2 from the deeper layer and outflow of CO_2 from the upper layer, if horizontal movement of CO_2 is not considered. CO_2 efflux on the surface occurred because of the CO_2 production in the soil, vertical gradient of CO_2 concentration with the opening on the surface, and diffusivity of the soil. The flux in any layer is the sum of production in this layer and flux from the deeper layer. Therefore, the CO_2 flux accumulates from the deeper layer to the surface because of production of CO_2 in all layers. If we assume a constant production of CO_2 from a certain depth to the surface, we can estimate CO_2 flux at the soil surface from flux at deeper layers that were derived from concentration measurements in the soil. In this study, we had only three layers of concentration measurements resulting in two fluxes at two depths. To estimate the soil surface flux based on non-linear relationship between flux and depth we would need accurate measurements at more and deeper layers of the soil as well as near the soil surface. In addition, our assumption of constant diffusivity at 0–30 cm may be biased. More measurements of soil moisture and bulk density at various layers of the soil and verification of diffusivity models in the field are suggested.

High CO_2 concentrations and gradients may results in high surface CO_2 efflux if there is no considerable change in soil CO_2 diffusivity. For example, D153 had higher CO_2 concentration at 16 cm in the control than that on D183 (Fig. 2a and b), and also had higher CO_2 efflux than D183 (Fig. 3a and b). However, high CO_2 concentrations may not necessarily result in high CO_2 efflux due to change in diffusivity. CO_2 concentration at 16 cm in the control plot on D153 was similar to that on D244 (Fig. 2a and d), but CO_2 efflux was much lower on D153 than D244 (Fig. 3a and d) because of differences

in CO_2 gradients and diffusivity between these two days.

Although CO_2 efflux from the surface soil is the combined results from CO_2 production in various layers of the soil and transport of CO_2 from the deeper layer of the soil to the surface with complex controls, it is still possible for us to use environmental variables to directly simulate surface CO_2 flux without considering the biological processes. Our empirical relationship between CO_2 efflux and soil temperature, moisture and precipitation explained 88% (in the control) and 68% (in the trenched plot) of the variation in measurements if the rain pulses were also considered.

4.2. CO_2 efflux with and without roots

Soil CO_2 efflux showed a clear diurnal pattern in the trenched plot but not in the control. The first reason may be due to a lower diurnal temperature range in the control resulting from shading of tree and shrub canopy. The open trenched plot had higher temperature ranges than in the control (Fig. 4). The second reason may be due to the influence of photosynthesis on respiration in the control plot. Root respiration accounted for over half of total soil respiration in the growing season. It was reported that root-dominated soil respiration may be influenced by photosynthesis but with a time lag of 7–12 h in the foothills of the Sierra Nevada (Tang et al., 2005a). The peak respiration influenced by photosynthesis during the course of a day could be later than the peak of photosynthesis due to the time needed for the translocation of photosynthate from leaves to roots. This influence may offset the response of soil respiration to soil temperature in the control plot, resulting a decoupling of soil respiration with soil temperature. In the trenched plot, because there was no influence from roots, the correlation between CO_2 efflux and temperature in the diurnal pattern was strong.

4.3. Controls on soil respiration

Our soil respiration model indicated that daily mean soil temperature and moisture explained most of the daily variation in soil respiration, with better correlation in the control than the trenched plot. Soil moisture had two opposite effects on soil respiration. We can derive from the coefficients for the quadratic term in Eq. (9) that when soil moisture was less than 0.21 $m^3\ m^{-3}$ for the control or 0.34 $m^3\ m^{-3}$ for the trenched plot, soil respiration responded positively to soil moisture; when soil moisture was greater than the above values, soil respiration responded negatively to soil moisture. This pattern was also observed in earlier studies at this site (Tang et al., 2005b) and in a nearby savanna with the similar Mediterranean climate (Tang and Baldocchi, 2005) with the similar value of optimum soil moisture. The difference of the optimum soil moisture between the control and trenched plot may be due to the influence of roots in the control, which may have different moisture preference from microbes.

Our bi-variable model indicates that temperature sensitivity of soil respiration changes with moisture. When moisture changes, the response of soil respiration to temperature varies. Soil respiration responds exponentially to soil temperature only when soil moisture holds constant. When soil moisture is a constant (e.g. within a few days in the summer), Q_{10} (temperature sensitivity) equalled 1.47 for the control plot and 1.76 for the trenched plot. The Q_{10} value in the control is consistent with a previous study using the chamber method ($Q_{10} = 1.55$) (Tang et al., 2005b). Higher Q_{10} for heterotrophic respiration in the trenched plot than the control may suggest lower Q_{10} for root respiration. This result disagrees with the reports of Boone et al. (1998) and Lavigne et al. (2003) that showed root respiration had a higher Q_{10} value than soil heterotrophic respiration in a temperate forest and in a boreal forest. This disagreement is probably due to the acclimation of root respiration to temperature sensitivity (Atkin and Tjoelker, 2003; Loveys et al., 2003) at this site with very high soil temperature and low soil moisture in the growing season.

4.4. Rain pulses

The pulse of soil respiration responding to rain cannot be simply explained by the variation of soil moisture measured at 0–30 cm. The increase in water content in the very surface layer of the soil or the litter layer, which are often unable to be recorded by soil moisture sensors buried in deeper layers, may cause the rapid increase in respiration. The pulse effect after wetting of the soil was originally reported by Birch (1958, 1959) in laboratory experiments. It was recently observed in the field using chamber measurements (Yuste et al., 2003; Liu et al., 2002; Lee et al., 2002), eddy covariance measurements (Lee et al., 2004), and soil CO_2 gradient measurements (Xu et al., 2004; Jassal et al., 2005). The mechanism explaining this rapid release of CO_2 to the atmosphere is not well understood (Halverson et al., 2000). The potential explanations include the release of intracellular solutes to the environment due to the disruption of cell membranes or cell lysis under the dramatic difference in water

potential after wetting or rain, and the rapid catabolism of low molecular weight carbohydrates or other labile carbon solutes to CO_2 (Halverson et al., 2000; Kieft et al., 1987; Fierer and Schimel, 2002).

4.5. Model results

Our model combined a subcomponent using soil temperature and moisture as drivers and another subcomponent simulating the exponential decay of pulses in response to rain to estimate the annual sum of soil respiration. The annual soil respiration (1184 g C m^{-2} y^{-1}) in 2003 reported here is higher than an earlier study (Misson et al., 2005) conducted at this site that reported soil respiration of 1035 g C m^{-2} y^{-1} in 2002. In addition to the interannual variability in climate, two reasons may explain this higher value of soil respiration. First, this plantation experienced fast growth after a forest thinning in 2000. The fast growth and expansion of roots may increase the total soil respiration in 2003. The second reason is due to the incorporation of the rain pulse effect. The earlier study (Misson et al., 2005) observed the pulse effect in the field but did not incorporate it in a modeling framework. Thus, the model may underestimate respiration by neglecting the rain pulses. Two pulses in this study covered 46 days with sum of soil respiration of 301 g C m^{-2}, or 25% of annual sum. Without the rain pulse component, our model would result in 1052 g C m^{-2} y^{-1} of annual soil respiration, or 132 g C m^{-2} y^{-1} (11%) less than the model with the rain pulse component. The large proportion of respiration pulses indicates that the magnitude and timing of the pulse effect will significantly influence the annual carbon budget. The summer rain events in late July and August in 2003 have not been observed in years from 1998 to 2002. These rain events, combined with high soil temperature in July and August, may result in higher pulses in 2003 than those that occurred in other years when the first rain usually occurred in October or November. However, more significant respiration pulses may not necessarily result in higher annual sum of CO_2 efflux. In a neutral ecosystem with net ecosystem exchange (NEE) close to 0, annual soil CO_2 efflux equals annual input of carbon into the soil including litter input and carbon released from roots (root respiration plus root decomposition). Thus, the pulse effect, which may shift the timing of CO_2 efflux over a year, may not change the annual sum of CO_2 efflux. However, this young plantation was in its fast growth period with more carbon uptake than release (Misson et al., 2005). The litterfall was also greater than decomposition, observed from the accumulation of debris layer (O horizon). Therefore, higher respiration pulses due to earlier rain events in 2003 may increase the annual sum of CO_2 efflux holding other condition unchanged.

The annual sum of CO_2 efflux in this study was higher than that from another young ponderosa pine forest in Oregon with a similar climate (Irvine and Law, 2002). Irvine and Law (2002) reported an annual CO_2 efflux of 427–519 g C m^{-2} y^{-1} from a naturally generated young pine forest with a similar age, but a lower LAI than our site; they also reported significant rain pulse effects. The higher value of soil respiration in this study is consistent with the higher ecosystem respiration (∼1267 g C m^{-2} y^{-1}) (Misson et al., 2005) in this site than the Oregon site (∼835 g C m^{-2} y^{-1}) (Law et al., 2001b) both measured with the eddy covariance method in 1999–2000.

4.6. Root respiration

We found the F_r/F ratio varied with seasons with a much higher value in the growing season (0.56) than in the non-growing season (0.16). The F_r/F ratio may also vary with years. The F_r/F ratio in the growing season is higher than a previous study that estimated a constant F_r/F ratio of 0.47 in the growing season of 1998 using the root biomass measurement method (Xu et al., 2001). The higher F_r/F ratio in 2003 than in 1998 may be due to the expanding of roots, particularly after the thinning. In addition, different methodologies in these two studies may also explain the different result in the F_r/F ratio.

We used the root exclusion (trenching) method to estimate heterotrophic respiration and thus to derive root respiration in the control plot. Root respiration was derived from the model that took into account the differences of soil temperature and moisture between the trenched plot and the control plot. However, our result may overestimate root respiration since heterotrophic respiration may be underestimated in the control plot. Heterotrophic respiration in the control might be larger than in the trenched plot due to the difference in soil organic matter, nutrients, and microbial community. However, this difference could be small because saturated recent litterfall and debris from previous clear cutting covered both the control and trenched plot. We did not find significant differences in total organic carbon and nitrogen content in the soil (0–20 cm) between the control and trenched plot. Therefore, the error associated with the difference of heterotrophic respiration in the control and trenched plot could be small. Another potential error in estimating root respiration is related to the concern of the root residues

(roots killed by trenching) in the trenched plot, which may cause overestimation of heterotrophic respiration in the trenched plot (Epron et al., 1999b). Ewel et al. (1987) and Bowden et al. (1993) reported that the influence of fine root residues in the trenched plot was small 4 months after trenching. This study reported data from the trenched plot 2 years after trenching. Therefore, we assumed that the influence from fine root residues was negligible. We also ignored the possible coarse root residues in the trenched plot.

5. Conclusion

The CO_2 gradient method provides a useful tool for continuously measuring soil respiration. The algorithm we provided in this paper allows us to compute soil surface CO_2 efflux from measurements of CO_2 concentrations and modeling of soil diffusivity. The gradient method enables us to examine the diurnal and seasonal variation in soil respiration. With complementary chamber measurements, we are able to estimate soil respiration from point measurements to the ecosystem level. Combining the trenching method, we are able to determine soil respiration with and without the root component, and thus estimate root respiration and the temporal variation in the ratio of root respiration to total soil respiration. Measured CO_2 concentrations in the soil were mainly determined by CO_2 production and soil diffusivity, while soil surface CO_2 efflux correlated well with soil temperature and moisture. Both CO_2 concentrations and soil surface CO_2 efflux varied between the control and trenched plots, indicating the influence from tree roots.

Soil respiration immediately and dramatically increased in response to the summer rain after a long drought in the Mediterranean-type ecosystem. The respiration pulses significantly influenced the annual sum of soil respiration. We simulated seasonal variation in soil respiration including the rain pulse effect using the variables of soil temperature, soil moisture and precipitation. The model explained 88% (in the control) and 68% (in the trenched plot) of measurements data. Without considering the rain pulses, the model would underestimate the annual soil respiration by 11%. The annual sum of soil respiration in 2003 was estimated as 1184 g C m^{-2} y^{-1}, with root respiration of 524 g C m^{-2} y^{-1}.

Acknowledgements

We thank Dennis Baldocchi for his insightful comments for this research, Sierra Pacific Industries for allowing us to perform this research on their property and the Blodgett Forest crew for their invaluable support. This research was supported by the Kearney Foundation of Soil Science and the Office of Science, Biological and Environmental Research Program (BER), US Department of Energy, through the Western Regional Center of the National Institute for Global Environmental Change (NIGEC) under Cooperative Agreement No. DE-FCO2-03ER63613. Financial support does not constitute an endorsement by DOE of the views expressed in this article.

References

Atkin, O.K., Tjoelker, M.G., 2003. Thermal acclimation and the dynamic response of plant respiration to temperature. Trends Plant Sci. 8 (7), 343–351.

Baldocchi, D.D., Meyers, T.P., 1991. Trace gas-exchange above the floor of a deciduous forest. 1. Evaporation and CO_2 efflux. J. Geophys. Res. -Atmos. 96 (D4), 7271–7285.

Birch, H.F., 1958. The effect of soil drying on humus decomposition and nitrogen availability. Plant Soil 10 (1), 9–31.

Birch, H.F., 1959. Further observations on humus decomposition and nitrification. Plant Soil 11 (3), 262–286.

Boone, R.D., Nadelhoffer, K.J., Canary, J.D., Kaye, J.P., 1998. Roots exert a strong influence on the temperature sensitivity of soil respiration. Nature 396 (6711), 570–572.

Bowden, R.D., Nadelhoffer, K.J., Boone, R.D., Melillo, J.M., Garrison, J.B., 1993. Contributions of aboveground litter, belowground litter, and root respiration to total soil respiration in a temperate mixed hardwood forest. Can. J. For. Res. 23 (7), 1402–1407.

Cox, P.M., Betts, R.A., Jones, C.D., Spall, S.A., Totterdell, I.J., 2000. Acceleration of global warming due to carbon-cycle feedbacks in a coupled climate model. Nature 408 (6809), 184–187.

Davidson, E.A., Belk, E., Boone, R.D., 1998. Soil water content and temperature as independent or confounded factors controlling soil respiration in a temperate mixed hardwood forest. Glob. Change Biol. 4 (2), 217–227.

Davidson, E.A., Savage, K., Verchot, L.V., Navarro, R., 2002. Minimizing artifacts and biases in chamber-based measurements of soil respiration. Agric. For. Meteorol. 113 (1–4), 21–37.

Drewitt, G.B., Black, T.A., Nesic, Z., Humphreys, E.R., Jork, E.M., Swanson, R., Ethier, G.J., Griffis, T., Morgenstern, K., 2002. Measuring forest floor CO_2 fluxes in a Douglas-fir forest. Agric. For. Meteorol. 110 (4), 299–317.

Epron, D., Farque, L., Lucot, E., Badot, P.M., 1999a. Soil CO_2 efflux in a beech forest: dependence on soil temperature and soil water content. Ann. For. Sci. 56 (3), 221–226.

Epron, D., Farque, L., Lucot, E., Badot, P.M., 1999b. Soil CO_2 efflux in a beech forest: the contribution of root respiration. Ann. For. Sci. 56 (4), 289–295.

Ewel, K.C., Cropper Jr., W.P., Gholz, H.L., 1987. Soil carbon dioxide evolution in Florida (USA) slash pine plantations: II Importance of root respiration. Can. J. For. Res. 17 (4), 330–333.

Fierer, N., Schimel, J.P., 2002. Effects of drying-rewetting frequency on soil carbon and nitrogen transformations. Soil Biol. Biochem. 34 (6), 777–787.

Goh, K.M., 2004. Carbon sequestration and stabilization in soils: Implications for soil productivity and climate change. Soil Sci. Plant Nutr. 50 (4), 467–476.

Goldstein, A.H., Hultman, N.E., Fracheboud, J.M., Bauer, M.R., Panek, J.A., Xu, M., Qi, Y., Guenther, A.B., Baugh, W., 2000. Effects of climate variability on the carbon dioxide, water, and sensible heat fluxes above a ponderosa pine plantation in the Sierra Nevada (CA). Agric. For. Meteorol. 101 (2–3), 113–129.

Goulden, M.L., Crill, P.M., 1997. Automated measurements of CO_2 exchange at the moss surface of a black spruce forest. Tree Physiol. 17 (8–9), 537–542.

Halverson, L.J., Jones, T.M., Firestone, M.K., 2000. Release of intracellular solutes by four soil bacteria exposed to dilution stress. Soil Sci. Soc. Am. J. 64 (5), 1630–1637.

Hanson, P.J., Edwards, N.T., Garten, C.T., Andrews, J.A., 2000. Separating root and soil microbial contributions to soil respiration: a review of methods and observations. Biogeochemistry 48 (1), 115–146.

Healy, R.W., Striegl, R.G., Russell, T.F., Hutchinson, G.L., Livingston, G.P., 1996. Numerical evaluation of static-chamber measurements of soil–atmosphere gas exchange: identification of physical processes. Soil Sci. Soc. Am. J. 60 (3), 740–747.

Hirano, T., Kim, H., Tanaka, Y., 2003. Long-term half-hourly measurement of soil CO_2 concentration and soil respiration in a temperate deciduous forest. J. Geophys. Res. -Atmos. 108 (D20), 4631, doi: 10.1029/2003JD003766.

Irvine, J., Law, B.E., 2002. Contrasting soil respiration in young and old-growth ponderosa pine forests. Glob. Change Biol. 8 (12), 1183–1194.

Jassal, R., Black, A., Novak, M., Morgenstern, K., Nesic, Z., Gaumont-Guay, D., 2005. Relationship between soil CO_2 concentrations and forest-floor CO_2 effluxes. Agric. For. Meteorol. 130 (3–4), 176–192.

Jones, H.G., 1992. Plants and Microclimate: A Quantitative Approach to Environmental Plant Physiology. Cambridge University Press, New York, 51.

Kieft, T.L., Soroker, E., Firestone, M.K., 1987. Microbial biomass response to a rapid increase in water potential when dry soil is wetted. Soil Biol. Biochem. 19 (2), 119–126.

King, J.A., Harrison, R., 2002. Measuring soil respiration in the field: An automated closed chamber system compared with portable IRGA and alkali absorption methods. Commun. Soil Sci. Plant Anal. 33 (3–4), 403–423.

Kirschbaum, M.U.F., 2000. Will changes in soil organic carbon act as a positive or negative feedback on global warming? Biogeochemistry 48 (1), 21–51.

Lal, R., 2004. Soil carbon sequestration to mitigate climate change. Geoderma 123 (1–2), 1–22.

Lavigne, M.B., Boutin, R., Foster, R.J., Goodine, G., Bernier, P.Y., Robitaille, G., 2003. Soil respiration responses to temperature are controlled more by roots than by decomposition in balsam fir ecosystems. Can. J. For. Res. 33 (9), 1744–1753.

Law, B.E., Baldocchi, D.D., Anthoni, P.M., 1999. Below-canopy and soil CO_2 fluxes in a ponderosa pine forest. Agric. For. Meteorol. 94 (3–4), 171–188.

Law, B.E., Kelliher, F.M., Baldocchi, D.D., Anthoni, P.M., Irvine, J., Moore, D., Van Tuyl, S., 2001a. Spatial and temporal variation in respiration in a young ponderosa pine forests during a summer drought. Agric. For. Meteorol. 110 (1), 27–43.

Law, B.E., Thornton, P.E., Irvine, J., Anthoni, P.M., Van Tuyl, S., 2001b. Carbon storage and fluxes in ponderosa pine forests at different developmental stages. Glob. Change Biol. 7 (7), 755–777.

Lee, M.-S., Nakane, K., Nakatsubo, T., Mo, W.-H., Koizumi, H., 2002. Effects of rainfall events on soil CO_2 flux in a cool temperate deciduous broad-leaved forest. Ecol. Res. 17 (3), 401–409.

Lee, X., Wu, H.J., Sigler, J., Oishi, C., Siccama, T., 2004. Rapid and transient response of soil respiration to rain. Glob. Change Biol. 10 (6), 1017–1026.

Liang, N.S., Inoue, G., Fujinuma, Y., 2003. A multichannel automated chamber system for continuous measurement of forest soil CO_2 efflux. Tree Physiol. 23 (12), 825–832.

Liang, N.S., Nakadai, T., Hirano, T., Qu, L.Y., Koike, T., Fujinuma, Y., Inoue, G., 2004. In situ comparison of four approaches to estimating soil CO_2 efflux in a northern larch (*Larix kaempferi* Sarg.) forest. Agric. For. Meteorol. 123 (1–2), 97–117.

Liu, X.Z., Wan, S.Q., Su, B., Hui, D.F., Luo, Y.Q., 2002. Response of soil CO_2 efflux to water manipulation in a tall grass prairie ecosystem. Plant Soil 240 (2), 213–223.

Livingston, G.P., Hutchinson, G.L., 1995. Enclosure-based measurement of trace gas exchange: applications and sources of error. In: Matson, P.A., Harriss, R.C. (Eds.), Biogenic Trace Gases: Measuring Emissions from Soil and Water. Blackwell Scientific, London, pp. 14–51.

Loveys, B.R., Atkinson, L.J., Sherlock, D.J., Roberts, R.L., Fitter, A.H., Atkin, O.K., 2003. Thermal acclimation of leaf and root respiration: an investigation comparing inherently fast- and slow-growing plant species. Glob. Change Biol. 9 (6), 895–910.

Meyer, W.S., Reicosky, D.C., Barrs, H.D., Shell, G.S.G., 1987. A portable chamber for measuring canopy gas exchange of crops subject to different root zone conditions. Agron. J. 79 (1), 181–184.

Misson, L., Panek, J.A., Goldstein, A.H., 2004. A comparison of three approaches to modeling leaf gas exchange in annually drought-stressed ponderosa pine forests. Tree Physiol. 24 (5), 529–541.

Misson, L., Tang, J., Xu, M., McKay, M., Golstein, A.H., 2005. Influences of recovery from clear-cut, climate variability, and thinning on the carbon balance of a young ponderosa pine plantation. Agric. For. Meteorol. 130 (3–4), 207–222.

Moldrup, P., Olesen, T., Yamaguchi, T., Schjonning, P., Rolston, D.E., 1999. Modeling diffusion and reaction in soils. IX. The Buckingham–Burdine–Campbell equation for gas diffusivity in undisturbed soil. Soil Sci. 164 (8), 542–551.

Norman, J.M., Garcia, R., Verma, S.B., 1992. Soil surface CO_2 fluxes and the carbon budget of a grassland. J. Geophys. Res. -Atmos. 97 (D17), 18845–18853.

Raich, J.W., Potter, C.S., Bhagawati, D., 2002. Interannual variability in global soil respiration 1980–1994. Glob. Change Biol. 8 (8), 800–812.

Raich, J.W., Schlesinger, W.H., 1992. The global carbon-dioxide flux in soil respiration and its relationship to vegetation and climate. Tellus B 44 (2), 81–99.

Rayment, M.B., Jarvis, P.G., 2000. Temporal and spatial variation of soil CO_2 efflux in a Canadian boreal forest. Soil Biol. Biochem. 32 (1), 35–45.

Reichstein, M., Rey, A., Freibauer, A., Tenhunen, J., Valentini, R., Banza, J., Casals, P., Cheng, Y.F., Grunzweig, J.M., Irvine, J., Joffre, R., Law, B.E., Loustau, D., Miglietta, F., Oechel, W., Ourcival, J.M., Pereira, J.S., Peressotti, A., Ponti, F., Qi, Y., Rambal, S., Rayment, M., Romanya, J., Rossi, F., Tedeschi, V., Tirone, G., Xu, M., Yakir, D., 2003. Modeling temporal and large-scale spatial variability of soil respiration from soil water availability, temperature and vegetation productivity indices. Global Biogeochem. Cy. 17 (4), 1104, doi: 10.1029/2003GB002035.

Russell, C.A., Voroney, R.P., Black, T.A., Blanken, P.D., Yang, P.C., 1998. Carbon dioxide efflux from the floor of a boreal aspen forest. II. Evaluation of methods-verification by infra-red analysis of a dynamic closed chamber. Can. J. Soil Sci. 78 (2), 311–316.

Scott, A., Crichton, I., Ball, B.C., 1999. Long-term monitoring of soil gas fluxes with closed chambers using automated and manual systems. J. Environ. Qual. 28 (5), 1637–1643.

Tang, J., Baldocchi, D.D., 2005. Spatial-temporal variation of soil respiration in an oak–grass savanna ecosystem in California and its partitioning into autotrophic and heterotrophic components. Biogeochemistry 73 (1), 183–207.

Tang, J., Baldocchi, D.D., Qi, Y., Xu, L., 2003. Assessing soil CO_2 efflux using continuous measurements of CO_2 profiles in soils with small solid-state sensors. Agric. For. Meteorol. 118 (3–4), 207–220.

Tang, J., Baldocchi, D.D., Xu, L., 2005a. Tree photosynthesis modulates soil respiration on a diurnal time scale. Glob. Change Biol. 11 (8), 1298–1304.

Tang, J., Qi, Y., Xu, M., Misson, L., Goldstein, A.H., 2005b. Forest thinning and soil respiration in a ponderosa pine plantation in the Sierra Nevada. Tree Physiol. 25 (1), 57–66.

Treonis, A.M., Wall, D.H., Virginia, R.A., 2002. Field and microcosm studies of decomposition and soil biota in a cold desert soil. Ecosystems 5 (2), 159–170.

Trumbore, S.E., Chadwick, O.A., Amundson, R., 1996. Rapid exchange between soil carbon and atmospheric carbon dioxide driven by temperature change. Science 272 (5260), 393–396.

Xu, L., Baldocchi, D.D., Tang, J., 2004. How soil moisture, rain pulses, and growth alter the response of ecosystem respiration to temperature. Global Biogeochem. Cy. 18 (GB4002), doi: 10.1029/2004GB002281.

Xu, M., DeBiase, T.A., Qi, Y., Goldstein, A., Liu, Z.G., 2001. Ecosystem respiration in a young ponderosa pine plantation in the Sierra Nevada Mountains, California. Tree Physiol. 21 (5), 309–318.

Xu, M., Qi, Y., 2001. Soil-surface CO_2 efflux and its spatial and temporal variations in a young ponderosa pine plantation in northern California. Glob. Change Biol. 7 (6), 667–677.

Yuste, J.C., Janssens, I.A., Carrara, A., Meiresonne, L., Ceulemans, R., 2003. Interactive effects of temperature and precipitation on soil respiration in a temperate maritime pine forest. Tree Physiol. 23 (18), 1263–1270.